ChemPubSoc Europe

DOI: 10.1002/cmdc.202000011

CHEMMEDCHEM Communications

Small-Molecule Inhibitors of METTL3, the Major Human Epitranscriptomic Writer

Rajiv K. Bedi,[a] Danzhi Huang,[a] Stefanie A. Eberle,[a, b] Lars Wiedmer,[a] Pawel Śledź,*[a] and Amedeo Caflisch*[a]

The RNA methylase METTL3 catalyzes the transfer of a methyl group from the cofactor S-adenosyl-L-methionine (SAM) to the N^6 atom of adenine. We have screened a library of 4000 analogues and derivatives of the adenosine moiety of SAM by high-throughput docking into METTL3. Two series of adenine derivatives were identified *in silico*, and the binding mode of six of the predicted inhibitors was validated by protein crystallography. Two compounds, one for each series, show good ligand efficiency. We propose a route for their further development into potent and selective inhibitors of METTL3.

The discovery of post-transcriptional modifications of RNA and their regulatory role in gene expression has revealed additional layer of control of cellular fate. By altering the structure, stability, and molecular recognition of RNA transcripts these modifications have been shown to regulate a variety of cellular processes,[1] including stem cell differentiation and stress response.[2] The level of RNA modifications is regulated by writer and eraser proteins (i.e., enzymes that install and remove the modification, respectively), and any misregulation of this process could drive development of disease.[3] Thus, proteins involved in epitranscriptomic regulation have been attracting attention as targets in drug discovery efforts.[1a,4] S-adenosyl-L-methionine (SAM)-dependent RNA methyltransferases constitute one important class of epitranscriptomic writers for which no chemical structure of small molecule inhibitors has been reported to date except for Sinefungin (PDB ID: 6Y4G), a natural nucleoside related to SAM.

Here we report a cofactor mimicking approach to search for inhibitors of the major cellular epitranscriptomic writer, METTL3 (methyltransferase-like protein 3). METTL3 installs the m^6A modification by transferring a methyl group from the cofactor SAM to the position N^6 of adenine within the mRNA recognition sequence DRACH (D=A, G or U; R=G or A; H=A, C or U).[5] As m^6A is the most prevalent post-transcriptional internal modification of mRNA with potential influence on a variety of diseases (ranging from cancer to viral infections), there is demand for small molecule inhibitors to study its role and provide leads for therapeutic development.

Adenosine (**1**), one of the two moieties of SAM (the other being L-methionine), is a SAM-competitive inhibitor of METTL3 with IC_{50} of about 500 μM (Table 1). Not surprisingly, the binding mode of adenosine overlaps with the adenosine moiety of both SAM and its product S-adenosyl-L-homocysteine (SAH, Figure 1a). We sought to use the adenosine scaffold of SAM to display different chemical moieties towards the putative m^6A binding pocket. To this end, we selected a library of nearly 4000 compounds containing the adenosine moiety or its mimics from commercially available sources. These compounds were docked by the program AutoDock[6] into the SAM binding site of METTL3 which was kept rigid. A total of 120,000 poses were filtered for the presence of two hydrogen bonds with the backbone NH groups of Ile378 and Asn549 which are involved as donors in hydrogen bonds to the N1 and N3 atoms, respectively, of the adenine of SAM. As an additional filter, poses with two or more buried polar groups not involved in hydrogen bonds with METTL3 were discarded.[7] A total of 70 compounds were purchased for experimental validation. They contained adenine (or a close analogue of adenine) and a sugar or sugar mimic attached to it, with possibly additional moiety extending from the sugar to reach the RNA-binding site.

The 70 compounds were tested in two orthogonal assays. The biochemical assay makes use of an m^6A reader YTH domain for detection of the reaction product and homogeneous time-resolved fluorescence (HTRF).[8] The predicted binding mode was validated by X-ray crystallography (Figures 1 and 2) in a competitive soaking experiment against SAH (see Supplementary Information for details on the experimental methods). Seven of the 70 compounds were hits in one or both of the assays (Table 1). They belong to two chemical series, N-substituted amide of ribofuranuronic acid analogues of adenosine (compounds **2**–**6**), and adenosine mimics with a six-member ring instead of ribose (compounds **7** and **8**). The inhibitors **2** and **3** could be validated in both assays (Table 1). Two compounds were identified only in the enzyme inhibition assay while the crystal structure of their complex with METTL3 could not be obtained (compounds **6** and **7**). For the remaining three binders (compounds **4**, **5**, and **8**) we could solve the crystal structure in the complex with METTL3 (Figure 3), yielding however no measurable affinity in the HTRF assay at the highest concentration tested (500 μM).

[a] R. K. Bedi, Dr. D. Huang, S. A. Eberle, Dr. L. Wiedmer, Dr. P. Śledź, Prof. A. Caflisch
Department of Biochemistry, University of Zürich
Winterthurerstrasse 190, 8057 Zürich (Switzerland)
E-mail: caflisch@bioc.uzh.ch
p.sledz@bioc.uzh.ch

[b] S. A. Eberle
Current address: Department of Biomedical Sciences
Faculty of Health and Medical Sciences, University of Copenhagen
Blegdamsvej 3, 2200 Copenhagen (Denmark)

Supporting information for this article is available on the WWW under https://doi.org/10.1002/cmdc.202000011

© 2020 Wiley-VCH Verlag GmbH & Co. KGaA, Weinheim

Table 1. Chemical structures of METTL3 inhibitors and inhibitory potency measured by the reader-based HTRF assay. The unit of the ligand efficiency (LE) is kcal/mol per number of non-hydrogen atoms. The single-dose inhibition gives the remaining enzyme activity in the presence of the test compound and is expressed as a percentage of the DMSO control.

Compound	2D structure	Remaining activity at 500 μM	IC_{50} [μM]	LE	PDB ID (Resol. [Å])
1 (adenosine)	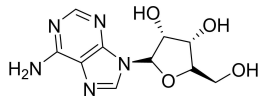	63%	495	0.24	6TTP (2.0)
2	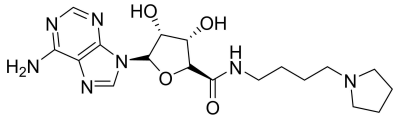	−3%	8.7	0.24	6TTT (2.3)
3	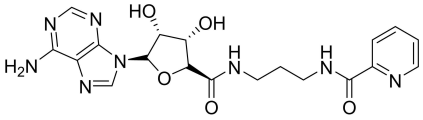	38%	332	0.15	6TTV (2.14)
4	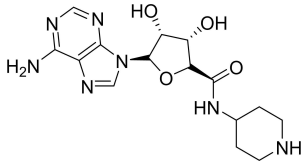	NS	ND	–	6TTW (2.2)
5	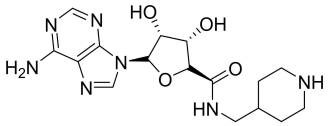	NS	>250	<0.18	6TTX (2.0)
6	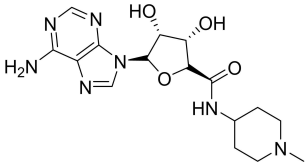	18%	65	0.21	-
7	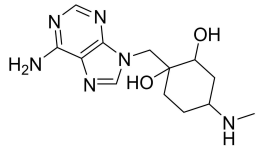	20%	98	0.26	-
8	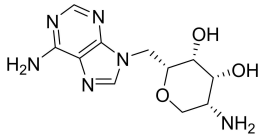	107%	>250	<0.25	6TU1 (2.31)

Compound **7** is a single stereoisomer of unknown configuration. NS = not soluble at 500 μM. ND = not determined.

The crystal structures of the METTL3 complex with the ribofuranuronic acid analogues of adenosine (compounds **2**–**5**) and the adenosine analogue with the tetrahydropyran ring (compound **8**) show a conserved binding mode with the adenine moiety engaged in the two aforementioned hydrogen bonds with the backbone NH groups of Ile378 and Asn549 (Figures 1b and 2b). The position of the ribose ring is also conserved while the tetrahydropyran of compound **8** is slightly displaced because of the additional methylene linker (Figure 3). The side chains in the SAM binding site show essentially identical orientation in all structures except for the tip of Arg536 whose guanidinium group adopts variable orientations (Figure 2a). The most disordered region in the SAM binding site is the loop segment Ile400-Gly407 (Figure 2b).

N-substituted amides of ribofuranuronic acid analogues of adenosine constitute an attractive modification, as their synthesis can be streamlined to yield new analogues as starting points for ligand development. The compounds **2** and **3** can be traced in the electron density only up to the amide moiety. Lack of electron density for the rest of the molecule can be attributed to disorder of their flexible tail which consists of four and three methylene groups, respectively. Compounds **4** and **5** both contain a piperidine ring, and differ by only one carbon atom in the linker between piperidine and amide. Their piperidine is stabilized in the space between the two active site loops by van der Waals interactions with the side chains of Pro397 and Ser511, and ionic interactions with Asp395 and Glu481 (Figure 3). Lack of measurable binding affinity for compounds **4** and **5** is consistent with the electrostatic

© 2020 Wiley-VCH Verlag GmbH & Co. KGaA, Weinheim

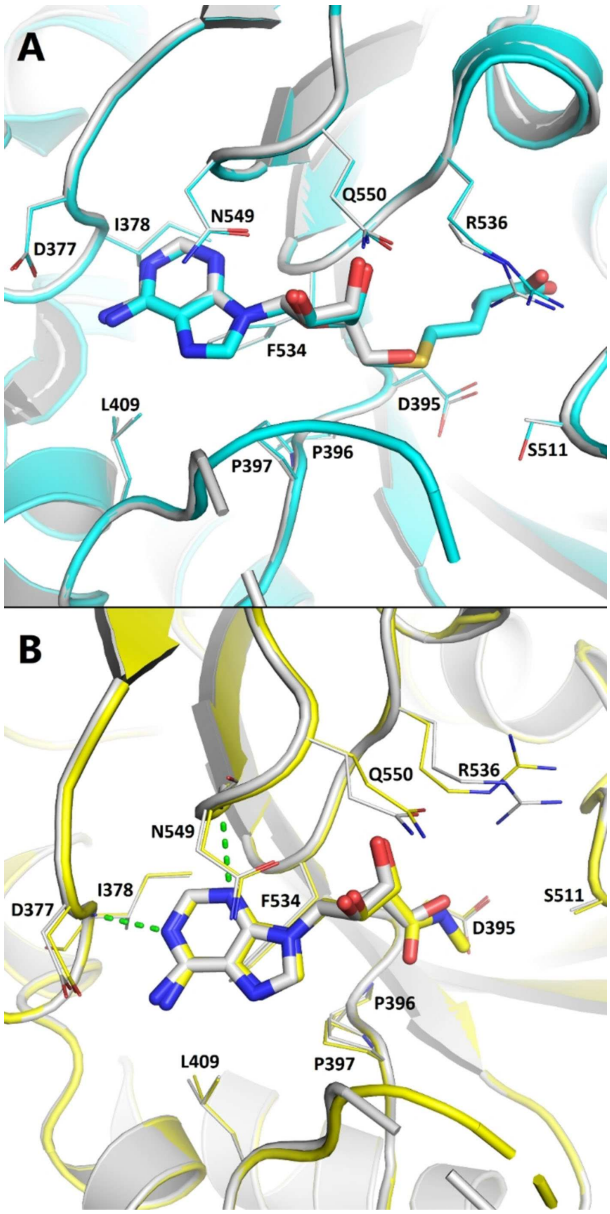

Figure 1. Conserved binding mode of mimics of the adenosine moiety of the SAM cofactor. (**A**) Structural overlap of the complexes of METTL3 with SAH (carbon atoms in cyan, PDB code 5L6D) and adenosine (gray, 6TTP). (**B**) Structural overlap of the complexes with adenosine (gray) and the part of compound **2** that can be fitted in the electron density (yellow, 6TTT).

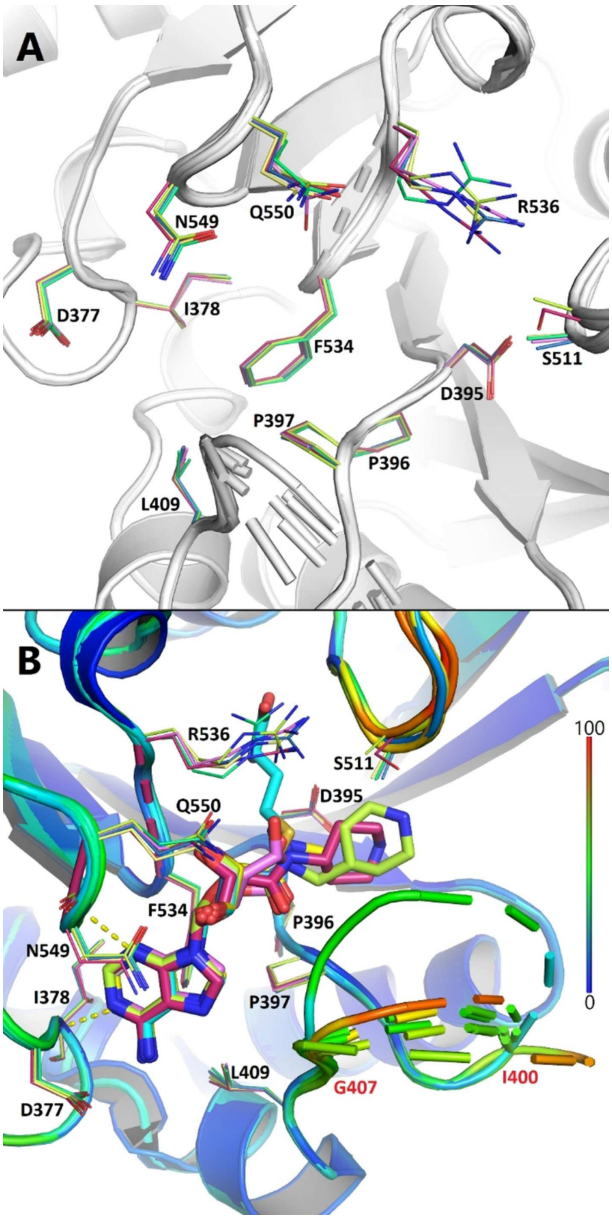

Figure 2. Binding site conservation and loop flexibility in the holo structures of METTL3. (**A**) Except for Arg536 the orientation of the side chains in the SAM pocket is conserved in the six holo structures. (**B**) Structural overlap of SAH (cyan) and the five inhibitors **2**, **3**, **4**, **5**, and **8**. The backbone is colored according to *B* factors (from blue to red, legend on the right). Broken segments of the Ile400-Gly407 loop indicate lack of electron density.

repulsion due to the side chain amino group of Lys513, and the electrostatic desolvation of Asp395 and Lys513. Compound **6**, an N-methylated derivative of **4**, shows higher potency with IC_{50} of about 65 μM which is likely a consequence of additional van der Waals interactions by its methyl group and/or differences in the pK_a value of secondary and tertiary amino groups. While it was not possible to solve the crystal structure of inhibitor **6** in the complex with METTL3 and attribute the affinity gain to any new interactions, it is likely that exploring SAR of these series will lead to more potent inhibitors.

The two hits with a six-member ring open the possibilities of designing inhibitors that do not contain the ribose moiety. Compound **7** has favorable ligand efficiency, but its binding mode could not be revealed. We were however successful in obtaining the binding mode of a close analogue, compound **8**. As mentioned above, the tetrahydropyran of compound **8** is slightly displaced with respect to the ribose ring of adenosine and the adenosine-based inhibitors because of the additional methylene linker. The primary amino group of inhibitor **8** is involved in an ionic interaction with the side chain of Asp395. It also forms polar interactions with the backbone carbonyl group of Asp395 and Phe534 (Figure 3).

© 2020 Wiley-VCH Verlag GmbH & Co. KGaA, Weinheim

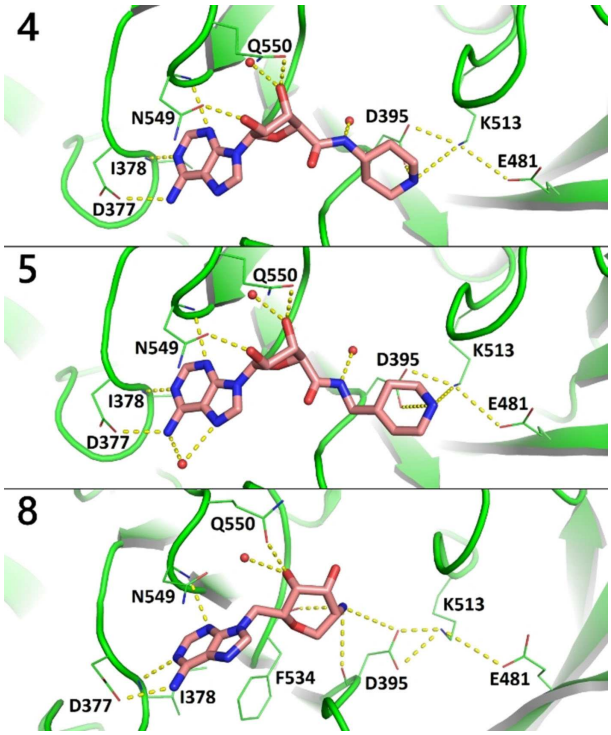

Figure 3. Crystal structures of METTL3 (green, ribbon model) in complex with compounds **4**, **5**, and **8** (carbon atoms in salmon). The PDB codes are 6TTW, 6TTX, and 6TU1, respectively. Polar contacts (yellow, dashed lines) and water molecules in contact with the inhibitors (red spheres) are shown.

In conclusion, high-throughput docking into the SAM-binding site and protein X-ray crystallography have allowed us to identify and structurally characterize the first small molecule inhibitors of METTL3, the key human epitranscriptomic writer. The adenosine derivative **2** has low μM potency in the HTRF assay and good ligand efficiency (Table 1). While adenosine analogues are often criticized as potential therapeutic agents due to their poor cellular permeability properties and promiscuity of binding, their medicinal chemistry optimization to clinical candidate can be carried out, as demonstrated by pinometostat which is in clinical trials.[9] We have also shown that the ribose of adenosine can be replaced by other ring systems, expanding the portfolio of potential modifications.

Recently, bisubstrate inhibitors have been synthesized that combine the structural features of nucleic acid substrate as well as SAM cofactor.[10] Such molecules have been shown to mimic the binding mode of both adenine to be methylated and SAM methyl-donor cofactor in bacterial methyltransferases. It has also been proposed that by extending the inhibitors to RNA binding site, selectivity over other SAM-utilizing enzymes can be attained. Therefore, bisubstrate inhibitors based on compounds **2** or **7** as SAM mimic should be considered for the development of chemical probes for METTL3.

Acknowledgements

We thank Dr. Aymeric Dolbois and Dr. Elena Omori for interesting discussions, Beat Blattmann for help with the setup of the liquid handler, and the staff at the Swiss Light Source, Paul Scherrer Institute for assistance in data collection. This work was supported by a grant of the Swiss National Science Foundation to AC and an Innovation Project grant from Innosuisse (Swiss Innovation Agency) as well as an Entrepreneur Fellowship in Biotechnology of the University of Zurich to PS. We also thank BaseLaunch (an initiative of BaselArea.swiss) for financial support.

Conflict of Interest

The authors declare no conflict of interest.

Keywords: Methyltransferase · m6A · Docking · protein crystallography · HTRF · METTL3/METTL14

[1] a) S. Lin, J. Choe, P. Du, R. Triboulet, R. I. Gregory, *Mol. Cell* **2016**, *62*(3), 335–345; b) C. R. Alarcon, H. Lee, H. Goodarzi, N. Halberg, S. F. Tavazoie, *Nature* **2015**, *519*(7544), 482–485; c) X. Wang, Z. Lu, A. Gomez, G. C. Hon, Y. Yue, D. Han, Y. Fu, M. Parisien, Q. Dai, G. Jia, B. Ren, T. Pan, C. He, *Nature* **2014**, *505*(7481), 117–120; d) X. Wang, B. S. Zhao, I. A. Roundtree, Z. Lu, D. Han, H. Ma, X. Weng, K. Chen, H. Shi, C. He, *Cell* **2015**, *161*(6), 1388–1399; e) W. Xiao, S. Adhikari, U. Dahal, Y. S. Chen, Y. J. Hao, B. F. Sun, H. Y. Sun, A. Li, X. L. Ping, W. Y. Lai, X. Wang, H. L. Ma, C. M. Huang, Y. Yang, N. Huang, G. B. Jiang, H. L. Wang, Q. Zhou, X. J. Wang, Y. L. Zhao, Y. G. Yang, *Mol. Cell* **2016**, *61*(4), 507–519.

[2] a) J. Zhou, J. Wan, X. Gao, X. Zhang, S. R. Jaffrey, S. B. Qian, *Nature* **2015**, *526*(7574), 591–594; b) T. Chen, Y. J. Hao, Y. Zhang, M. M. Li, M. Wang, W. Han, Y. Wu, Y. Lv, J. Hao, L. Wang, A. Li, Y. Yang, K. X. Jin, X. Zhao, Y. Li, X. L. Ping, W. Y. Lai, L. G. Wu, G. Jiang, H. L. Wang, L. Sang, X. J. Wang, Y. G. Yang, Q. Zhou, *Cell Stem Cell* **2015**, *16*(3), 289–301; c) P. J. Batista, B. Molinie, J. Wang, K. Qu, J. Zhang, L. Li, D. M. Bouley, E. Lujan, B. Haddad, K. Daneshvar, A. C. Carter, R. A. Flynn, C. Zhou, K. S. Lim, P. Dedon, M. Wernig, A. C. Mullen, Y. Xing, C. C. Giallourakis, H. Y. Chang, *Cell Stem Cell* **2014**, *15*(6), 707–719; d) Y. Wang, Y. Li, J. I. Toth, M. D. Petroski, Z. Zhang, J. C. Zhao, *Nat. Cell Biol.* **2014**, *16*(2), 191–198; e) S. T. Qi, J. Y. Ma, Z. B. Wang, L. Guo, Y. Hou, Q. Y. Sun, *J. Biol. Chem.* **2016**, *291*(44), 23020–23026; f) S. Geula, S. Moshitch-Moshkovitz, D. Dominissini, A. A. Mansour, N. Kol, M. Salmon-Divon, V. Hershkovitz, E. Peer, N. Mor, Y. S. Manor, M. S. Ben-Haim, E. Eyal, S. Yunger, Y. Pinto, D. A. Jaitin, S. Viukov, Y. Rais, V. Krupalnik, E. Chomsky, M. Zerbib, I. Maza, Y. Rechavi, R. Massarwa, S. Hanna, I. Amit, E. Y. Levanon, N. Amariglio, N. Stern-Ginossar, N. Novershtern, G. Rechavi, J. H. Hanna, *Science* **2015**, *347*(6225), 1002–1006.

[3] a) G. Zheng, J. A. Dahl, Y. Niu, P. Fedorcsak, C. M. Huang, C. J. Li, C. B. Vagbo, Y. Shi, W. L. Wang, S. H. Song, Z. Lu, R. P. Bosmans, Q. Dai, Y. J. Hao, X. Yang, W. M. Zhao, W. M. Tong, X. J. Wang, F. Bogdan, K. Furu, Y. Fu, G. Jia, X. Zhao, J. Liu, H. E. Krokan, A. Klungland, Y. G. Yang, C. He, *Mol. Cell* **2013**, *49*(1), 18–29; b) K. D. Meyer, S. R. Jaffrey, *Nat. Rev. Mol. Cell Biol.* **2014**, *15*(5), 313–326; c) J. Liu, Y. Yue, D. Han, X. Wang, Y. Fu, L. Zhang, G. Jia, M. Yu, Z. Lu, X. Deng, Q. Dai, W. Chen, C. He, *Nat. Chem. Biol.* **2014**, *10*(2), 93–95; d) G. Jia, Y. Fu, X. Zhao, Q. Dai, G. Zheng, Y. Yang, C. Yi, T. Lindahl, T. Pan, Y. G. Yang, C. He, *Nat. Chem. Biol.* **2011**, *7*(12), 885–887; e) N. Liu, T. Pan, *Nat. Struct. Mol. Biol.* **2016**, *23*(2), 98–102.

[4] a) C. M. Connelly, M. H. Moon, J. S. Schneekloth Jr., *Cell Chem. Biol.* **2016**, *23*(9), 1077–1090; b) Y. Li, R. K. Bedi, L. Wiedmer, D. Huang, P. Sledz, A. Caflisch, *J. Chem. Theory Comput.* **2019**, *15*(12), 7004–7014; c) D. P. Patil, B. F. Pickering, S. R. Jaffrey, *Trends Cell Biol.* **2018**, *28*(2), 113–127; d) X. Wang, C. He, *RNA Biol.* **2014**, *11*(6), 669–672; e) P. A. Boriack-Sjodin, S. Ribich, R. A. Copeland, *Nat. Rev. Drug Discovery* **2018**, *17*(6), 435–453; f) H. Shi, J. Wei, C. He, *Mol. Cell* **2019**, *74*(4), 640–650.

© 2020 Wiley-VCH Verlag GmbH & Co. KGaA, Weinheim

[5] a) K. D. Meyer, Y. Saletore, P. Zumbo, O. Elemento, C. E. Mason, S. R. Jaffrey, *Cell* **2012**, *149*(7), 1635–1646; b) D. Dominissini, S. Moshitch-Moshkovitz, M. Salmon-Divon, N. Amariglio, G. Rechavi, *Nat. Protoc.* **2013**, *8*(1), 176–189.
[6] G. M. Morris, R. Huey, W. Lindstrom, M. F. Sanner, R. K. Belew, D. S. Goodsell, A. J. Olson, *J. Comput. Chem.* **2009**, *30*(16), 2785–2791.
[7] H. Zhao, D. Huang, *PLoS One* **2011**, *6*(6), e19923.
[8] L. Wiedmer, S. A. Eberle, R. K. Bedi, P. Sledz, A. Caflisch, *Anal. Chem.* **2019**, *91*(4), 3078–3084.
[9] E. M. Stein, G. Garcia-Manero, D. A. Rizzieri, R. Tibes, J. G. Berdeja, M. R. Savona, M. Jongen-Lavrenic, J. K. Altman, B. Thomson, S. J. Blakemore, S. R. Daigle, N. J. Waters, A. B. Suttle, A. Clawson, R. Pollock, A. Krivtsov, S. A. Armstrong, J. DiMartino, E. Hedrick, B. Lowenberg, M. S. Tallman, *Blood* **2018**, *131*(24), 2661–2669.
[10] S. Oerum, M. Catala, C. Atdjian, F. Brachet, L. Ponchon, P. Barraud, L. Iannazzo, L. Droogmans, E. Braud, M. Etheve-Quelquejeu, C. Tisne, *RNA Biol.* **2019**, *16*(6), 798–808.

Manuscript received: January 9, 2020
Revised manuscript received: February 28, 2020
Version of record online: ■■, ■■■

© 2020 Wiley-VCH Verlag GmbH & Co. KGaA, Weinheim

COMMUNICATIONS

On your METTL: High-throughput docking into the SAM-binding site and protein X-ray crystallography have allowed us to identify and characterize the first small-molecule inhibitors of METTL3, the key human epitranscriptomic writer. Two compounds showed good ligand efficiency, and we propose a route for their development into potent, selective METTL3 inhibitors.